Advances in Science and Technology Research Journal

Advances in Science and Technology Research Journal 2024, 18(3), 99–110
https://doi.org/10.12913/22998624/185961
ISSN 2299-8624, License CC-BY 4.0

Received: 2023.11.27
Accepted: 2024.03.11
Published: 2024.04.20

Screw Extrusion as a Scalable Technology for Manufacturing Carbon Nanotube-Filled Polylactide Composites

Daniel Kaczor[1,2*], Krzysztof Bajer[2], Aneta Raszkowska Kaczor[2], Grzegorz Domek[1], Paweł Szroeder[3]

[1] Faculty of Mechatronics, Kazimierz Wielki University, Kopernika 1, 85-074 Bydgoszcz, Poland
[2] Łukasiewicz Research Network, Institute for Engineering of Polymer Materials and Dyes, Marii Skłodowskiej-Curie 55, 87-100 Toruń, Poland
[3] Faculty of Physics, Kazimierz Wielki University, Powstańców Wielkopolskich 2, 85-090 Bydgoszcz, Poland
* Corresponding author's e-mail: kaczor.daniel.piotr@gmail.com

ABSTRACT

The bottleneck in the widespread use of carbon multiwall nanotube polymer composites is the lack of manufacturing technology that can be used on an industrial scale. In this article, we describe a two-step composite manufacturing technology based on screw extrusion that produces composites characterizing with good dispersion of carbon nanotube filler in polylactide matrix. The first stage involved the fabrication of highly filled masterbatches of 25 wt% of carbon nanotubes. In the second stage, by screw extrusion of the masterbatch mixture with neat polymer, we obtained homogeneous composites with the target filler concentration. The resulting composites with nanotube content ranging from 0.1 to 2 wt%. Mechanical tests including static tension, tensile strength, tensile modulus, three-point bending and impact strength has shown that optimal concentration of the carbon nanotube filler is ranged between 0.5 and 1 wt%. Samples were examined also by SEM, FTIR-ATR, DSC and MFR methods.

Keywords: extrusion, polylactide, composite, masterbatch, carbon nanotube.

INTRODUCTION

The increased interest in environmentally friendly technologies in the last few years has drawn the attention of industry and scientists to replacing traditional polymers obtained from petroleum products with their counterparts derived from renewable sources. One such polymer that is enjoying growing interest is polylactide [1]. It is one of the oldest, most interesting and has many applications in the automotive [2, 3], agriculture [4, 5], medicine [6, 7], electronics [8, 9], packaging [10, 11] and others industry. Currently, PLA holds the first position on the market from biodegradable polymers [12]. In 1932, Wallace Carothers, an employee of DuPont, was the first to synthesize polylactide. He obtained a short chain polymer by heating lactic acid under vacuum [13]. Since 1960s, polylactide has been used in medicine and pharmacy as absorbable implants, sutures and in controlled drug release [14, 15].

The advantages of polylactide are its good mechanical properties and the possibility of biodegradation. Unfortunately, this polymer also has its weaknesses. Low impact strength, susceptibility to thermal deformation and low gas barrier limit its wider use [16]. These and other properties can be improved by adding natural or glass fibres, other biodegradable polymers and fillers to polylactide [17, 18, 19, 20, 21].

The addition of carbon nanotubes (CNT) is one of the alternatives to improve the properties of the composite. CNTs were discovered in soot resulting from the evaporation of a graphite electrode in an electric arc in 1991 by Sumio Iijima [22]. A distinction is made between singlewall nanotubes (SWCNT), which are a single layer of graphene rolled into a cylinder, and multiwall

nanotubes (MWCNT), which are made of many coaxial cylinders. Nanotubes with diameters ranging from one to several tens of nanometres and lengths ranging from several tens to hundreds of micrometres have a very high aspect ratio. CNTs have excellent mechanical properties. Tensile strength reaching values between 25–66 GPa [23, 24] and a Young's modulus greater than 1 TPa [25, 26]. The excellent mechanical properties of the carbon nanofiller are responsible for the increased strength of PLA composites with carbon nanotubes [27]. The strengthening effect depends of the percentage CNT content and the quality of their dispersion in polymer matrix. In particular, the presence of CNT agglomerates leads to a reduction in mechanical performance [28]. The appropriate distribution of CNTs in the polymer matrix can be achieved by selecting optimal processing conditions influenced by the filler content [29]. Article focuses on the extrusion process of PLA/CNT composites with filler content from 0.1 to 2 wt%. The target composites are obtained from our own masterbatch containing 25 wt% of multiwall carbon nanotubes. The masterbatch allows for precise dosing of small amounts of nanomaterials into the composite. We examined the obtained composites for filler dispersion and possible changes in the structure of the polymer matrix and the influence of MWCNT content on the melt flow rate and strength properties of the composites.

SAMPLE PREPARATION AND TEST METHODS

Materials

In our research, we used polylactide (PLA) produced by Total-Corbion (Gorinchen, Netherlands), available under the trade name Luminy® LX175, as the polymer matrix. The used PLA is characterized (according to data sheet) by density of 1.24 g/cm^3, stereochemical purity 96 % (L-isomer), residual monomer content of ≤0.3 %. Glass transition and melting temperature of LX175 is 60 °C and 155 °C, respectively. The polymer was used in two forms: powder, with a grain size of 100 to 600 μm to obtain masterbatch and in the form provided by the manufacturer – granules, for sample composites. Multiwall carbon nanotubes (MWCNT) purchased from The Institute of Carbon Technologies (Toruń, Poland) were used as the filler in obtained samples. The nanotubes have lengths in the range of 5 to 20 μm, diameters of 10 to 30 nm and a specific surface area of 80 m^2/g.

Composite production technology

The procedure of obtaining research samples was divided into two stages. In the initial stage, polymer masterbatch containing 25 wt% of carbon nanotubes was prepared. In second step, masterbatch was diluted to the target MWCNT content in the samples (from 0.1 to 2 wt%). Before extrusion, the raw materials and the obtained masterbatch were dried in a dryer for 8 h at 80 °C (dryer: POL-EKO SLW 180 STD, POL-EKO sp.k., Poland).

Masterbatch preparation

The polymer masterbatch was made by extruding pre-mixed PLA powder with 25 wt% MWCNT. For extrusion, a twin-screw, co-rotating Bühler BTSK extruder (Uzwil, Switzerland) was used with a screw diameter of 20 mm and a L/D (length to diameter) of 40. The extruder was equipped with a screw of the K3 configuration (Fig. 1). Used configuration is characterized by good mixing properties. Screw contains four zones responsible for mixing and grinding the extruded material. The first mixing zone contains KBW 90/2/15 and KBW 45/5/20 kneading elements. Following zones, in addition to the kneading elements, contain also return elements whose task is to retain the melted mixture in the mixing

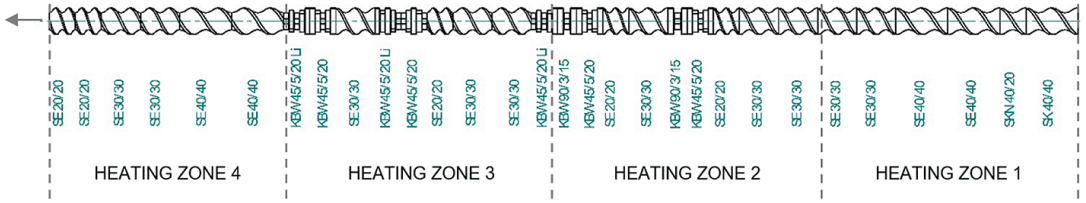

Figure 1. Screw configuration with marked heating zones of extruder, SK - feeding segments, SE - conveying segments, KBW - kneading elements, elements marked as Li - backward elements (angle/step/length in mm)

zone for longer to intensify mixing. The masterbatch was extruded at a screw rotation speed of 100 rpm and heating zone temperatures (from 1 to 4) of 170 °C, 175 °C, 180 °C, 185 °C and 185 °C (head). In order to get rid of MWCNT agglomerates, the masterbatch obtained after one extrusion was returned to the extruder. More information on the properties of highly filled polymer masterbatches can be found in our previous publications [30, 31].

Composite preparation

The tested samples containing from 0.1 to 2 wt% of MWCNT were made by mixing an appropriate amount of the masterbatch prepared in the first stage, containing 25 wt% of carbon nanotubes, with polylactide granules. The premix was extruded using a Bühler BTSK extruder equipped with a K3 screw. All composites were extruded at 150 rpm (screw speed) and a temperature of heating zones (from 1 to 4): 170 °C, 175 °C, 180 °C, 185 °C, 180 °C (head). During extrusion, stock temperature (T_t), main drive torque (M_0), power main drive (W), and efficiency (Y) were recorded. The tested samples were extruded, unlike the masterbatch, only once. Prepared samples: 0.1%MWCNT/PLA, 0.3%MWCNT/PLA, 0.5%MWCNT/PLA, 1.0%MWCNT/PLA, 2.0%MWCNT/PLA, containing 0.1, 0.3, 0.5, 1.0 and 2.0 wt% MWCNT, respectively. A sample extruded without the addition of filler was marked as PLA.

Material characterization

Microscopic analysis

In order to assess the dispersion, uniformity of distribution and the presence of agglomerates of the nanotube filler, the scanning electron microscopy (SEM) method was used. Images were recorded using a Hitachi SU8010 (Japan). The picture were taken after covering the sample surface with a thin layer of gold to increase its electrical conductivity and at an acceleration voltage of 5 and 10 kV and a working distance of 8 mm.

Spectroscope analysis

The impact of the extrusion process on the chemical structure of the polymer matrix was assessed using attenuated total reflectance infrared spectroscopy (FTIR-ATR). The Cary 630 spectrometer from Agilent Technology (Santa Clara, California, USA) equipped with a diamond crystal was used to record the spectra. Measuring range from 400 to 4000 cm^{-1} with spectral resolution < 2 cm^{-1} and signal-to-noise ratio (1 min, RMS) > 30000:1.

Thermal behavior analysis

The temperatures: T_g – glass transition, T_c – crystallization, T_{cc} – cold crystallization, T_m – melting and the enthalpies of these processes: ΔH_c – crystallization, ΔH_{cc} – cold crystallization, ΔH_m – melting were recorded using the differential scanning calorimetry (DSC) technique. A Mettler Toledo DSC1 calorimeter was used to record sample thermograms. Samples of raw polymer and composites with masses of 5 to 7 mg were placed in the in closed aluminium crucibles, measurements were carried out in an inert nitrogen atmosphere, with a gas flow over the sample of 60 cm^3/min and divided in three stages separated by two isothermal stages:

- heating 1:10 °C/min from 0 °C to 300 °C;
- first 5 min. isothermal stage (300 °C);
- cooling: 10 °C/min from 300 °C to 0 °C;
- second 5 min. isothermal stage (0 °C);
- heating 2: 10 °C/min from 0 °C to 300 °C.

To calculate the degree of crystallinity (X_c) at room temperature of the samples, the equation was used [32]:

$$X_C = \left(\frac{\Delta H_m - \Delta H_{cc}}{w\Delta H_m^0}\right) \cdot 100\% \qquad (1)$$

where: ΔH_m – melting enthalpy (J/g); ΔH_{cc} – cold crystallization enthalpy (J/g); ΔH^0_m – melting enthalpy of 100% crystalline PLA (93 J/g [33]), w – polymer fraction in the composite. The analysis was made in agreement with ISO 11357-(1–3) standards [34]. The accuracy of temperature determination was ± 0.8 °C and enthalpy ± 0.5 J/g.

Melt flow rate

The value of the melt flow rate (MFR) of the samples was measured using a Dynisco LMI 4003 capillary plastometer in accordance with the PN-EN ISO 1133 standard [35]. The analyses were made with a piston load of 2.16 kg, at 190 °C and a cutting time of 20 s. For all samples, the initial melting time was 300 s. Before measurements samples were dried by 4 hours in 80 °C.

Mechanical tests

Tests to determine mechanical properties in static tension included: tensile strength (σ_m), stress at brake (σ_b), strain at strength (ε_m), strain at break (ε_b), tensile modulus, modulus of elasticity under tension (Young's modulus, E_t). Three point bending tests were used to determine: flexural strength (σ_{fM}), flexural strain at flexural strength (ε_{fM}), flexural stress at conventional deflection (σ_{fc}), modulus of elasticity in flexure, flexural modulus (E_f). Impact strength was determined using the Charpy method (a_{cN}). Before starting the tests, the samples were conditioned for at least 24 hours at a temperature of 23 ± 1 °C and a humidity of 50 ± 5 %. Mechanical tests were also carried out under the same climatic conditions.

Specimens for mechanical tests were made using a Battenfeld Plus 35/75 UNILOG B2 injection moulding machine equipped with a screw with a diameter of 22 mm and a length of L/D 17 and three heating zones. In accordance with the PN-EN ISO 294-1 standard [36]. Two types of samples were prepared: shapes in the 1A mold ("dog bone" shape, 2 mm of thickness, for tensile strength tests) and beams 1eA (length/width/thickness – 80/10/4 mm, for three-point bending and Charpy test). Samples were injected at a temperature of 185 °C (all zones), using a dosing speed of 150 rpm, a dosing back pressure of 232 Bar, an injection pressure of 1627 Bar, with a screw rotation speed at injection stage from 126 (beginning of the injection process) to 210 rpm (end of the injection process), mold clamping pressure of 1627 Bar, pressing time 35 s, cooling time 20 s, mold temperature 40 °C, injection volume: 28.8 cm^3 for 1A specimens and 20.8 cm^3 for bars. Before injection, the granulates were dried for 4 hours at 80 °C in a POL-EKO SLW 180 STD dryer. Mechanical properties in static tension was performed in accordance with PN-EN ISO 527-(1-2) standard [37]. The TIRAtest 27025 (TIRA Maschinenbau GmbH, Germany) testing machine, equipped with a 3 kN measuring head, was used for the tests. Modulus was determine with stretching speed of 1.0 mm/min. 50 mm/min was used to record the remaining strength parameters. Gauge length: 50 mm. The results presented are the average of five repetitions. Three-point bending was performed using a TIRAtest 27025 machine, 3 kN measuring head, 64 mm of support spacing and 2 mm/ testing speed. Also in this case, showed values are the average of five repetitions. Measurements was performed in accordance with PN-EN ISO 178 [38]. Charpy impact testing was performed on the IMPats-15/50 test stand (ATSFAAR S.p.A., Italy). A hammer with impact energy of 1 J and velocity at impact of 2.90 m/s was used. Samples in the shape of 1eA with a notch were used for testing. Width under the notch 8 mm. The samples notches were done with the use of NOTCH VIS (CEAST) machine. After notching, specimens were conditioning by at least 16 hours in standard conditions. The tests were performed in accordance with the standard PN-EN ISO 179-1 [39]. The value given is the average of ten repetitions.

RESULTS

Sample preparation process analysis

Table 1 shows the processing values recorded during the extrusion of individual samples. The values of recorded extrusion parameters for individual samples did not differ significantly from each other. The small used filling of the composites did not change the values of the recorded parameters compared to the sample made of pure polylactide. No differences were observed between the set and actual extrusion temperature of all samples. All granulates containing MWCNTs were characterized by equal colour, gloss, and smooth external surfaces.

Microscopic analysis

Figure 2 shows SEM images of both the composites components: PLA powder and raw MWCNT filler, as well as the fracture surfaces of MWCNT/PLA masterbatch (25 wt% of

Table 1. Parameters recorded during extrusion

Sample	PLA	0.1%MWCNT/PLA	0.3%MWCNT/PLA	0.5%MWCNT/PLA	1.0%MWCNT/PLA	2.0%MWCNT/PLA
T_t [°C]	210	203	206	206	206	207
M_o [Nm]	21.5	22.1	21.8	22.1	21.8	20.5
W [kW]	0.63	0.63	0.65	0.64	0.64	0.61
Y [kg/h]	3.25	3.25	3.25	3.25	3.25	3.25

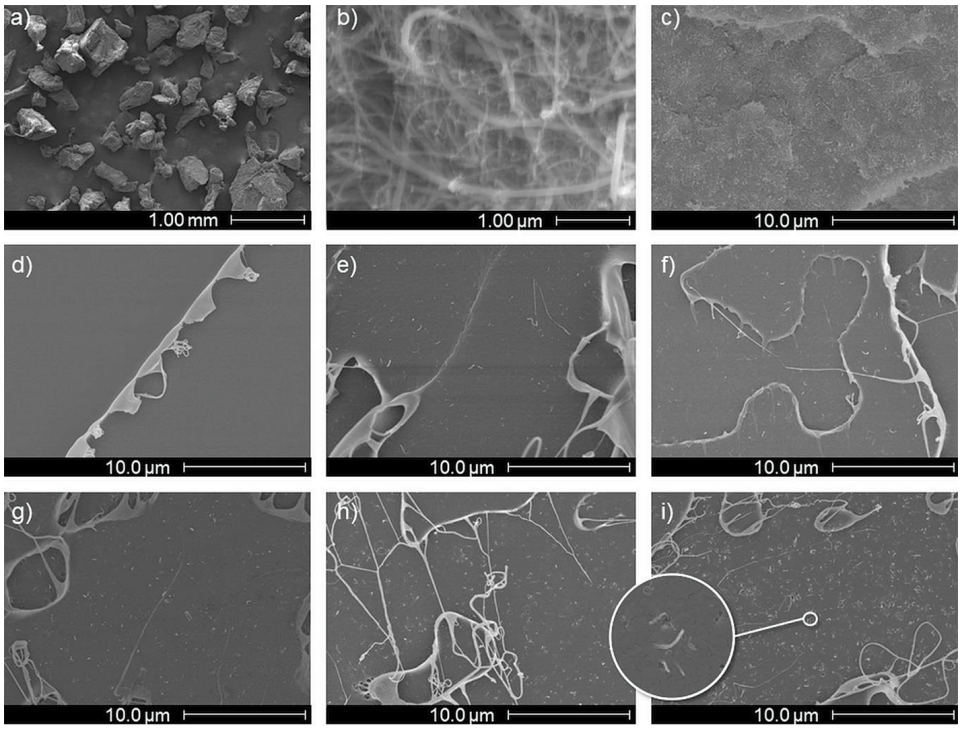

Figure 2. SEM images of: a) PLA powder, b) MWCNTs, c) fracture surface of MWCNT/PLA masterbatch, d) fracture surface of the extruded neat PLA, e-i) fracture surface of the extruded MWCNT/PLA composite containing 0.1, 0.3, 0.5, 1.0 and 2.0 wt% of MWCNTs, respectively

MWCNTs), extruded neat PLA and MWCNT/PLA composites. Morphology of the raw components agrees with the data provided by the suppliers. PLA grain sizes range from 100 to 600 µm (Figure 2a), the carbon filler is a tangle of cylindrical structures with a high aspect ratio (Figure 2b). On the surface of the MWCNT/PLA fracture, well dispersed nanotubes in the PLA matrix are visible (Figure 2c). The fractured surface of the neat PLA (Figure 2d) is smooth indicating an inherent brittle and stiffness of the material. The river marking along the crack shown in the image is accompanied with very short polymer threads. The morphology of the fracture surface changed after introduction of MWCNT filler into PLA matrix (Figure 2e-f). Although river markings are still visible at 0.1 and 0.3 wt% concentrations of nanotubes, however, the presence of much more elongated polymer threads on the surface of the breakthrough is significantly increased. In fracture surfaces of samples with MWCNT content higher than 0.5 wt%, the river markings disappeared and the length and number of PLA threads increased. PLA threads with lengths of tens of micrometres appeared in fracture surface of composite with 1.0 wt% concentration of MWCNTs. It is worth noting that the MWCNTs were distributed evenly in the composites and no cracks, holes or other types of structure discontinuities were observed in the polymer matrix.

Chemical structure analysis

Figure 3 shows a comparison of the FTIR-ATR spectra of the tested composite samples and neat PLA. All recorded spectra contain bands characteristic of polylactide. The crystalline and amorphous polymer phases are represented by bands located at 754 cm^{-1} and 866 cm^{-1} respectively [40]. C-CH_3 group stretching modes appears at 1041 cm^{-1}. The bands located at 1081 cm^{-1}, 1180 and 1266 cm^{-1} correspond to the bands of symmetric and asymmetric stretching of the C-O-C group. Rocking modes of CH_3 groups are visible at 1127 cm^{-1}. Symmetric bending modes of CH and CH_3 appear at 1361 and 1381 cm^{-1}. At 1451 cm^{-1} asymmetric bending modes of CH and CH_3 groups can be found. The C=O ester stretching modes occur at 1747 cm^{-1}. Bands, with low intensity, at 2944 and 2995 cm^{-1} are attribute to the CH_3 asymmetric stretching [41,42]. The position of individual bands in samples containing nanotubes corresponds to the position of these bands in original polylactide. The intensity of the bands

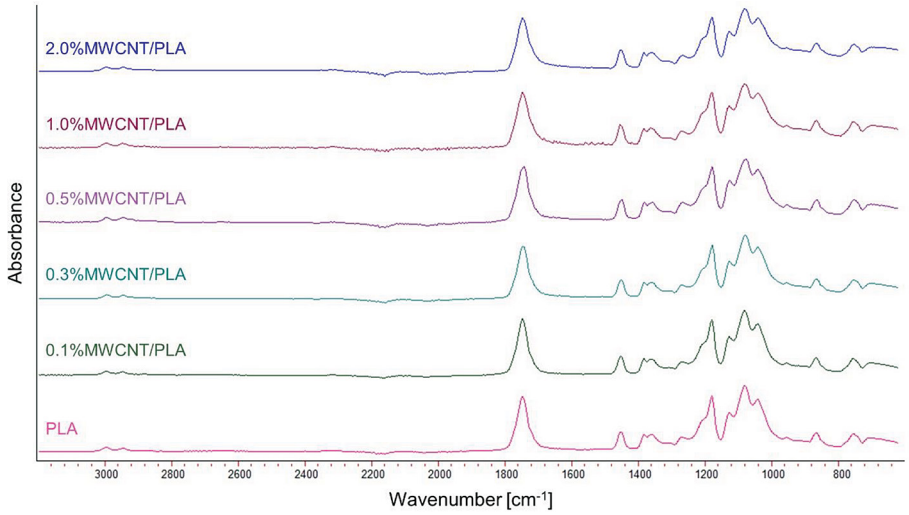

Figure 3. FTIR-ATR spectra of the tested samples and original PLA

recorded for the polymer matrix corresponding to carbonyl groups (1747 cm^{-1}) and ester groups (1081 and 1180 cm^{-1}) didn't change during extrusion. A change in the intensity (reduction) of these bands would indicate a shortening of the length of the polymer chains and thus its degradation [43]. This proves that the addition of carbon nanotubes did not cause degradation of the polymer matrix or their impact was minimal.

Thermal behaviour analysis

The results of the DSC analysis are shown in Table 2 and Figures 4–5. The first heating is used to erase the thermal history of the sample after the extrusion process. The transition recorded at the lowest temperature in the first heating thermograms was the endothermic glass transition. After exceeding this temperature, the polymer chains become movable. For composites with MWCNT, the temperature of this transition is 60 °C, which is the same value as for pure PLA. This means that the filler used in the tested range of content in the composite had no effect on limiting the mobility of polymer chains in this temperature [44]. The formation of an ordered domain from the amorphous domain was manifested by an exothermic peak at 115–129 °C in composites and 111 °C in the pure PLA thermograms. The T_{cc}^{1} temperature increases with increasing carbon nanotube content in the sample. The presence of MWCNT is

Table 2. Thermal parameters obtained by DSC

Sample	PLA	0.1%MWCNT/PLA	0.3%MWCNT/PLA	0.5%MWCNT/PLA	1.0%MWCNT/PLA	2.0%MWCNT/PLA
Heating 1						
T_g^1 [°C]	60.0	60.3	61.0	60.1	59.9	59.7
T_{cc}^1 [°C]	111.1	115.2	125.3	126.7	129.0	129.0
ΔH_{cc}^1 [J/g]	26.0	27.9	21.7	12.3	12.3	6.9
T_m^1 [°C]	151.6	152.7	155.5	154.3	155.9	154.6
ΔH_m^1 [J/g]	26.1	28.5	22.8	13.9	12.7	7.9
X_c^1 [%]	0	0	0	0	0	0
Heating 2						
T_g^2 [°C]	59.6	59.1	59.7	59.8	58.3	59.4
T_{cc}^2 [°C]	129.2	129.0	125.3	127.5	122.0	128.0
ΔH_{cc}^2 [J/g]	9.5	11.8	18.3	16.1	23.6	15.6
T_m^2 [°C]	150.0	150.0	149.3	149.1	147.8 153.6	150.3
ΔH_m^2 [J/g]	9.5	11.4	18.5	16.1	23.6	15.9
X_c^2 [%]	0	0	0	0	0	0

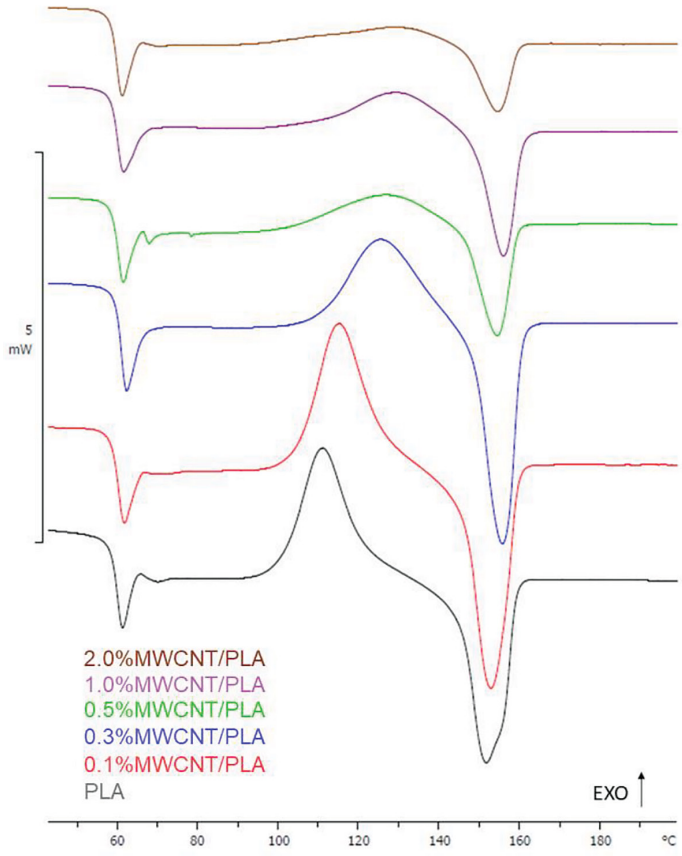

Figure 4. Heating 1 thermograms

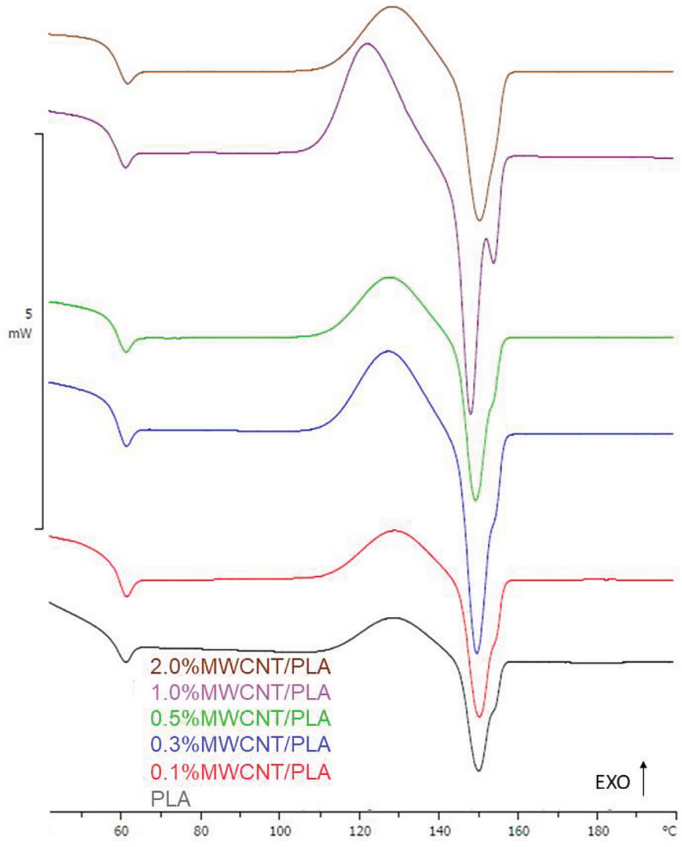

Figure 5. Heating 2 thermograms

responsible for the increase in the cold T_{cc}^{1}. In the process of crystallite formation, the filler had a negative effect on the mobility of polymer chains [44]. Changes in the enthalpy of cold crystallization were also visible. ΔH_{cc} also decreases with increasing MWCNT content in the sample. The quality of the formed crystallites was responsible for the change in the enthalpy of cold crystallization. The presence of filler limits the area in which crystals can grow. The result is the formation of small, imperfect crystallites whose T_{cc} is higher and ΔH_{cc} smaller than those of better structures [45]. The melting point recorded during the first heating for the composite samples was higher than for pure PLA. The quality of crystallites formed during cold crystallization was responsible for the simultaneous increase in T_{m}^{1} and decrease in ΔH_{m}^{1} of MWCNT samples [46].

During cooling of all samples, no effects related to polylactide crystallization were recorded. This confirms that crystallites cannot form while the sample was cooling. The ordered phase in the polymer was formed only during the heating of the sample from the molten phase. Therefore, PLA was not able to crystallize from the solid phase [47]. More information about the interaction of the filler with the polymer matrix was provided by the second heating. In the thermograms of the second heating, no major differences were recorded between the glass transition temperatures of the samples filled with MWCNTs and the sample without this additive. This means that the presence of the filler had no effect on the mobility of the polylactide chain [44]. For samples containing MWCNT, H_{cc}^{2} was higher and T_{cc}^{2} was lower compared to pure PLA. Carbon nanotubes influence the location of the exothermic cold crystallization peak. The decrease in the cold crystallization temperature and the increase in the enthalpy of this process indicate that MWCNTs can act as polylactide crystallization nuclei [48]. The melting peaks of the samples recorded in the second heating thermograms were asymmetric. For a sample containing 1% by weight MWCNT, a second peak emerged from this asymmetry. Two types of crystallites that differ in size and order are responsible for the appearance of the two melting peaks [49]. Qualitatively inferior crystallites (smaller, with a lesser degree of order) melt at a lower temperature and then recrystallize to a more stable form. The newly formed crystallites melt at a higher temperature [50]. All samples showed amorphous character.

Melt flow rate

Composites and reference sample melt flow rate values are show in Table 3. The mass melt flow rate is an expression of melt flowability, defined as the mass of molten polymer passing through a capillary of standardized diameter and length at a specified time and at a specified pressure applied by the weight. Because the MFR value is determined under constant load conditions, it can be considered as an extrusion rheometer representing a specific point on the shear stress versus shear rate curve. This value is directly correlated with the melt viscosity [51,52]. The measured MFR value of the extruded sample containing only polylactide (7.07 g/10 min) is similar to the value measured for polylactide in the form provided by the manufacturer (7.81 g/10 min). A sharp increase in the MFR value may indicate polymer degradation [53]. In such a case, the increase in flow and the decrease in the viscosity of the material are caused by the significant shortening (breaking) of the polymer chain as a result of high temperature and shear forces [54]. Since both values are close to each other, it can be assumed that the used processing conditions didn't affect (or the impact was minor) on degradation of the polymer. The MFR value of MWCNT samples decreased with increasing filler loading. The decrease in the MFR, samples melt viscosity, was caused by the presence of a solid filler and thus an increase in the flow resistance of the molten polymer [55].

Mechanical tests

Mechanical properties in static tension are shown in Table 4. The addition of MWCNT to the polylactide matrix resulted in an increase in both tensile strength and Young's modulus. All samples showed typical brittle fracture behaviour,

Table 3. MFR results for individual samples (standard deviation)

Sample	PLA	0.1%MWCNT/PLA	0.3%MWCNT/PLA	0.5%MWCNT/PLA	1.0%MWCNT/PLA	2.0%MWCNT/PLA
MFR [g/10 min]	7.07 (0.05)	4.53 (0.04)	4.15 (0.09)	3.59 (0.09)	3.17 (0.09)	2.90 (0.06)

Table 4. Mechanical properties – static tension (standard deviation)

Sample	PLA	0.1%MWCNT/PLA	0.3%MWCNT/PLA	0.5%MWCNT/PLA	1.0%MWCNT/PLA	2.0%MWCNT/PLA
σ_m [MPa]	62.5 (0.7)	63.8 (0.6)	65.1 (0,8)	65.8 (0.7)	68.9 (0.6)	67.7 (0.5)
σ_b [MPa]	60.8 (1.0)	63.8 (0.6)	64.5 (1.0)	65.8 (0.7)	68.7 (0.6)	67.7 (0.2)
ε_m [%]	4.2 (0.2)	3.9 (0.1)	4.0 (0.1)	4.1 (0.2)	4.0 (0.2)	3.9 (0.2)
ε_b [%]	4.5 (0.2)	3.9 (0.1)	4.1 (0.1)	4.1 (0.2)	4.1 (0.3)	3.9 (0.2)
E_t [MPa]	1982 (62)	2119 (101)	2120 (111)	2118 (78)	2279 (59)	2178 (102)

Table 5. Mechanical properties – three-point bending (standard deviation)

Sample	PLA	0.1%MWCNT/PLA	0.3%MWCNT/PLA	0.5%MWCNT/PLA	1.0%MWCNT/PLA	2.0%MWCNT/PLA
σ_{fm} [MPa]	97.0 (2.8)	99.0 (2.7)	94.6 (2.5)	97.4 (2.9)	98.9 (1.2)	96.1 (2.3)
σ_{fc} [MPa]	95.2 (2.6)	95.8 (4.4)	93.1 (2.5)	96.4 (3.0)	95.8 (1.7)	92.0 (2.3)
ε_{fm} [%]	4.3 (0.1)	4.3 (0.2)	4.2 (0.2)	4.3 (0.2)	4.3 (0.2)	4.4 (0.1)
E_f [MPa]	3290 (181)	3386 (128)	3116 (129)	3308 (56)	3208 (161)	3019 (44)

Table 6. Mechanical properties – impact strength (standard deviation)

Sample	PLA	0.1%MWCNT/PLA	0.3%MWCNT/PLA	0.5%MWCNT/PLA	1.0%MWCNT/PLA	2.0%MWCNT/PLA
a_{cN} [kJ/m^2]	2.73 (0.29)	2.86 (0.17)	2.90 (0.24)	3.01 (0.32)	2.90 (0.27)	2.78 (0.13)

without any visible yielding phenomenon. The best strength properties during static tensile tests were obtained for a sample containing 1 wt% of carbon nanotubes. For this sample, σ_m it changed by 10% and E_t by 15% compared to the PLA sample. The addition of carbon filler did not cause changes in elongation at the maximum recorded stress and at break. The strengthening effect, associated with excellent mechanical properties of MWCNT is responsible for improving the strength parameters [56, 57]. Most of the external loads are carried by the PLA matrix. Microcracks created during stretching initiate and spread in the polymer matrix of composites when the applied load exceeds its strength [58]. This phenomenon may explain the decrease in strength parameters in the sample containing 2 wt% MWCNT. A higher content of carbon nanotubes in this sample causes disturbances in the continuity of the polymer matrix and thus weakens the composite. Similar observations were recorded by other researchers [29, 48, 59]. Table 5 show results obtained from three-point bending tests. In the case of three-point bending, the addition of MWCNT had no effect on the test results. The corresponding values of the parameters recorded during the test for individual samples are similar to each other. Due to the nucleating properties of MWCNTs and thus the increase in the degree of crystallinity of polylactide, which results in an increase in the brittleness of composites made using them, a deterioration of properties could be expected during this test [28]. However, rapid specimens cooling during injection molding, which prevented crystallization of the polymer, resulted in no changes in bending strength. Impact strength results determined by the Charpy method are summarized in Table 6.

A slight upward trend can be seen in the impact strength results of the obtained samples after adding MWCNT to the PLA matrix. However, the change is so small (within the measurement error of the samples) that it is safer to say that this parameter has not deteriorated for the composites compared to original polylactide.

CONCLUSIONS

The feasibility of using screw extrusion technology to produce homogeneous biodegradable PLA composites filled with carbon nanotube was investigated. Commercial PLA and a masterbatch containing 25% MWCNTs were used as starting material. For samples with target concentrations of filler (0.0–2.0 wt%), no significant changes were observed in the mechanical parameters of the extrusion process, such as stock temperature, main drive torque and efficiency.

The fracture surface of the obtained composites was strongly influenced by the content of the MWCNT filler. Addition of the MWCNTs resulted in appearance of the PLA threads on the fracture surface and disappearing of cracks. MWCNTs were distributed evenly in the composites and no voids were found in the composites. Empty spaces and pores, the presence of which could be related to the appearance of CO or CO_2 in the sample, may indicate polymer degradation [60]. The results of the FTIR-ATR analysis indicate that the applied sample extrusion conditions had no or minimal effect on the degradation of polylactide. There were also no chemical changes in structure of polylactide after the addition of MWCNTs during the preparation of composite samples. In the tested samples, MWCNT showed a nucleating effect on the formation of polylactide crystallites during the second heating of the DSC analysis. However, rapid cooling of the samples after extrusion did not allow the formation of polymer crystallites in the composites and all samples showed an amorphous character. The presence of MWCNTs influenced the change in the viscosity of the composites. The change in the MFR value is caused by increased resistance to polymer flow resulting from the increasing content of solid filler in the composite. Carbon nanotubes had the greatest impact on the properties of the obtained composites on the results of mechanical tests. Where their small addition (1 wt%) resulted in an increase in tensile strength by 10% and Young's modulus by 15%, without deterioration of the other measured parameters.

Acknowledgments

This work is supported by the Ministry of Education and Science of the Republic of Poland as part of the 'Implementation doctorate' program (contract No. DWD/4/71/2020) and by the Faculty of Mechatronics of the Kazimierz Wielki University (funds from the subsidy for scientific research).

REFERENCES

1. Farah S, Anderson DG, Langer R. Physical and mechanical properties of PLA, and their functions in widespread applications — A comprehensive review. Advanced Drug Delivery Reviews 2016; 107: 367–392.
2. Hu RH, Ma ZG, Zheng S, Li YN, Yang GH, Kim HK. A fabrication process of high volume fraction of jute fiber/polylactide composites for truck liner. Int J Precis Eng Manuf 2012; 13(7): 1243–6.
3. Notta-Cuvier D, Odent J, Delille R, Murariu M, Lauro F, Raquez JM. Tailoring polylactide (PLA) properties for automotive applications: Effect of addition of designed additives on main mechanical properties. Polymer Testing 2014; 36: 1–9.
4. Sevostyanov MA, Kaplan MA, Nasakina EO, Shatova LA, Tsareva AM, Kolmakova AA. Development of a Biodegradable Polymer Based on High-Molecular-Weight Polylactide for Medicine and Agriculture: Mechanical Properties and Biocompatibility. Dokl Chem. 2020; 490(2): 36–39.
5. Tertyshnaya Y, Jobelius H, Olkhov A, Shibryaeva L, Ivanitskikh A. Polylactide Fiber Materials and their Application in Agriculture. Key Engineering Materials 2022; 910: 617–622.
6. Peres C, Matos AI, Conniot J, Sainz V, Zupančič E, Silva JM. Poly(lactic acid)-based particulate systems are promising tools for immune modulation. Acta Biomaterialia. 2017; 48: 41–57.
7. Sullivan MP, McHale KJ, Parvizi J, Mehta S. Nanotechnology: current concepts in orthopaedic surgery and future directions. The Bone & Joint Journal 2014; 96–B(5): 569–573.
8. Zhou J, Yu J, Bai D, Lu J, Liu H, Li Y. AgNW/stereocomplex-type polylactide biodegradable conducting film and its application in flexible electronics. J Mater Sci: Mater Electron. 2021; 32(5): 6080–6093.
9. Al-Attar H, Alwattar AA, Haddad A, Abdullah BA, Quayle P, Yeates SG. Polylactide-perylene derivative for blue biodegradable organic light-emitting diodes. Polymer International 2021; 70(1): 51–58.
10. Ahmed J, Mulla M, Jacob H, Luciano G, T.b. B, Almusallam A. Polylactide/poly(ε-caprolactone)/zinc oxide/clove essential oil composite antimicrobial films for scrambled egg packaging. Food Packaging and Shelf Life 2019; 21: 100355.
11. Ahmed J, Mulla MZ, Al-Zuwayed SA, Joseph A, Auras R. Morphological, barrier, thermal, and rheological properties of high-pressure treated co-extruded polylactide films and the suitability for food packaging. Food Packaging and Shelf Life 2022; 32:100812.
12. Androsch R, Schick C, Di Lorenzo ML. Kinetics of Nucleation and Growth of Crystals of Poly(l-lactic acid). Synthesis, Structure and Properties of Poly(lactic acid). Advances in Polymer Science 2017; 279.
13. Carothers WH, Dorough GL, Natta FJV. Studies of polymerization and ring formation. The reversible polymerization of six-membered cyclic esters. J Am Chem Soc. 1932; 54(2): 761–772.
14. Kawai F. Polylactic Acid (PLA)-Degrading Microorganisms and PLA Depolymerases. ACS Symposium Series 2010; 1043.
15. Avinc O, Khoddami A. Overview of Poly(lactic acid)

(PLA) Fibre. Fibre Chem. 2009; 41(6): 391–401.

16. Trivedi AK, Gupta MK, Singh H. PLA based biocomposites for sustainable products: A review. Advanced Industrial and Engineering Polymer Research 2023; 6(4): 382–395.
17. Mokhena TC, Sefadi JS, Sadiku ER, John MJ, Mochane MJ, Mtibe A. Thermoplastic Processing of PLA/Cellulose Nanomaterials Composites. Polymers 2018; 10(12): 1363.
18. Sun Y, Zheng Z, Wang Y, Yang B, Wang J, Mu W. PLA composites reinforced with rice residues or glass fiber—a review of mechanical properties, thermal properties, and biodegradation properties. J Polym Res. 2022; 29(10): 422.
19. Fu Z, Cui J, Zhao B, Shen SGF, Lin K. An overview of polyester/hydroxyapatite composites for bone tissue repairing. Journal of Orthopaedic Translation 2021; 28: 118–130.
20. Shahdan D, Rosli NA, Chen RS, Ahmad S, Gan S. Strategies for strengthening toughened poly(lactic acid) blend via natural reinforcement with enhanced biodegradability: A review. International Journal of Biological Macromolecules 2023; 251: 126214.
21. Nofar M, Sacligil D, Carreau PJ, Kamal MR, Heuzey MC. Poly (lactic acid) blends: Processing, properties and applications. International Journal of Biological Macromolecules 2019; 125: 307–60.
22. Iijima S. Helical microtubules of graphitic carbon. Nature 1991; 354(6348): 56–58.
23. Takakura A, Beppu K, Nishihara T, Fukui A, Kozeki T, Namazu T. Strength of carbon nanotubes depends on their chemical structures. Nat Commun. 2019; 10(1): 3040.
24. Zhang P, Su J, Guo J, Hu S. Influence of carbon nanotube on properties of concrete: A review. Construction and Building Materials 2023; 369: 130388.
25. Wu Z, Zhao Y, Yang K, Guan J, Wang S, Gu Y. Enhancing the Mechanical Performance of Fiber-Reinforced Polymer Composites Using Carbon Nanotubes as an Effective Nano-Phase Reinforcement. Advanced Materials Interfaces 2023; 10(3): 2201935.
26. Peng B, Locascio M, Zapol P, Li S, Mielke SL, Schatz GC. Measurements of near-ultimate strength for multiwalled carbon nanotubes and irradiation-induced crosslinking improvements. Nature Nanotech. 2008; 3(10): 626–631.
27. Zhou Y, Lei L, Yang B, Li J, Ren J. Preparation and characterization of polylactic acid (PLA) carbon nanotube nanocomposites. Polymer Testing 2018; 68: 34–38.
28. Vidakis N, Petousis M, Kourinou M, Velidakis E, Mountakis N, Fischer-Griffiths PE. Additive manufacturing of multifunctional polylactic acid (PLA)—multiwalled carbon nanotubes (MWCNTs) nanocomposites. Nanocomposites 2021; 7(1): 184–199.
29. Wang L, Qiu J, Sakai E, Wei X. The relationship between microstructure and mechanical properties of carbon nanotubes/polylactic acid nanocomposites prepared by twin-screw extrusion. Composites Part A: Applied Science and Manufacturing 2016; 89: 18–25.
30. Kaczor D, Bajer K, Domek G, Madajski P, Raszkowska-Kaczor A, Szroeder P. Influence of Extruder Plasticizing Systems on the Selected Properties of PLA/Graphite Composite. Acta Mechanica et Automatica 2022; 16(4): 316–324.
31. Kaczor D, Bajer K, Raszkowska-Kaczor A, Domek G, Madajski P, Szroeder P. The Influence of Multiple Extrusions on the Properties of High Filled Polylactide/Multiwall Carbon Nanotube Composites. Materials 2022; 15(24): 8958.
32. Batakliev T, Georgiev V, Kalupgian C, Muñoz PAR, Ribeiro H, Fechine GJM. Physico-chemical Characterization of PLA-based Composites Holding Carbon Nanofillers. Appl Compos Mater. 2021; 28(4): 1175–1192.
33. Kang H, Kim DS. A study on the crystallization and melting of PLA nanocomposites with cellulose nanocrystals by DSC. Polymer Composites 2023; 44(11): 7727–7736.
34. Standard PN-EN ISO 11357-(1-3):2016-2020 Tworzywa Sztuczne-Różnicowa Kalorymetria Skaningowa (DSC); Część 1: Zasady Ogólne; Część 2: Wyznaczanie Temperatury Zeszklenia i Stopnia Przejścia w Stan Szklisty; Część 3: Oznaczanie Temperatury Oraz Entalpii Topnienia i Krystalizacji. Polish Committe for Standardization 2016–2020.
35. Standard PN-EN ISO 1133-1:2011 Tworzywa Sztuczne-Oznaczanie Masowego Wskaźnika Szybkości Płynięcia (MFR) i Objętościowego Wskaźnika Szybkości Płynięcia (MVR) Tworzyw Termoplastycznych-Część 1: Metoda Standardowa. Polish Committe for Standardization: Warsaw 2011.
36. Standard PN-EN ISO 294-1:2017 Tworzywa sztuczne - Wtryskiwanie kształtek do badań z tworzyw termoplastycznych; Część 1: Zasady ogólne, formowanie uniwersalnych kształtek do badań i kształtek w postaci beleczek. Polish Committe for Standardization 2017.
37. Standard PN-EN ISO 527-1:2020-01 Oznaczanie właściwości mechanicznych przy statycznym rozciąganiu; Część 1: Zasady ogólne; Część 2: Warunki badań tworzyw sztucznych przeznaczonych do prasowania wtrysku i wytłaczania. Polish Committe for Standardization 2012–2020.
38. Standard PN-EN ISO 178:2019-06 Tworzywa sztuczne - Oznaczanie właściwości przy zginaniu. Polish Committe for Standardization 2019.
39. Standard PN-EN ISO 179-1:2010 Tworzywa sztuczne. Oznaczanie udarności metodą Charpy'ego; Część 1: Badanie nieinstrumentalne. Polish Committe for Standardization 2010.
40. Yadav N, Nain L, Khare SK. Studies on the

degradation and characterization of a novel metal-free polylactic acid synthesized via lipase-catalyzed polymerization: A step towards curing the environmental plastic issue. Environmental Technology & Innovation 2021; 24: 101845.

41. Yuniarto K, Purwanto YA, Purwanto S, Welt BA, Purwadaria HK, Sunarti TC. Infrared and Raman studies on polylactide acid and polyethylene glycol-400 blend. AIP Conference Proceedings 2016; 1725(1): 020101.
42. Kister G, Cassanas G, Vert M. Effects of morphology, conformation and configuration on the IR and Raman spectra of various poly(lactic acid)s. Polymer 1998; 39(2): 267–73.
43. Amorin NSQS, Rosa G, Alves JF, Gonçalves SPC, Franchetti SMM, Fechine GJM. Study of thermodegradation and thermostabilization of poly(lactide acid) using subsequent extrusion cycles. Journal of Applied Polymer Science 2014; 131(6): 40023
44. Usachev SV, Lomakin SM, Koverzanova EV, Shilkina NG, Levina II, Prut EV. Thermal degradation of various types of polylactides research. The effect of reduced graphite oxide on the composition of the PLA4042D pyrolysis products. Thermochimica Acta 2022; 712: 179227.
45. Mngomezulu ME, Luyt AS, John MJ. Morphology, thermal and dynamic mechanical properties of poly(lactic acid)/expandable graphite (PLA/EG) flame retardant composites. Journal of Thermoplastic Composite Materials 2019; 32(1): 89–107.
46. Memarian F, Fereidoon A, Ghorbanzadeh Ahangari M. The shape memory, and the mechanical and thermal properties of TPU/ABS/CNT: a ternary polymer composite. RSC Adv. 2016; 6(103): 101038–101047.
47. Xu Z, Niu Y, Yang L, Xie W, Li H, Gan Z. Morphology, rheology and crystallization behavior of polylactide composites prepared through addition of five-armed star polylactide grafted multiwalled carbon nanotubes. Polymer 2010; 51(3): 730–737.
48. Park SH, Lee SG, Kim SH. Isothermal crystallization behavior and mechanical properties of polylactide/carbon nanotube nanocomposites. Composites Part A: Applied Science and Manufacturing 2013; 46: 11–18.
49. Ahmed J, Mulla MZ, Vahora A, Bher A, Auras R. Polylactide/graphene nanoplatelets composite films: Impact of high-pressure on topography, barrier, thermal, and mechanical properties. Polymer Composites 2021; 42(6): 2898–2909.
50. Bartczak Z, Galeski A, Kowalczuk M, Sobota M, Malinowski R. Tough blends of poly(lactide) and amorphous poly([R,S]-3-hydroxy butyrate) – morphology and properties. European Polymer Journal 2013; 49(11): 3630–3641.
51. Luyt AS, Gasmi S. Influence of blending and blend morphology on the thermal properties and crystallization behaviour of PLA and PCL in PLA/PCL blends. J Mater Sci. 2016; 51(9): 4670–81.
52. Aliotta L, Gigante V, Geerinck R, Coltelli MB, Lazzeri A. Micromechanical analysis and fracture mechanics of Poly(lactic acid) (PLA)/Polycaprolactone (PCL) binary blends. Polymer Testing 2023; 121: 107984.
53. Kumar S, Ramesh MR, Doddamani M, Rangappa SM, Siengchin S. Mechanical characterization of 3D printed MWCNTs/HDPE nanocomposites. Polymer Testing 2022; 114: 107703.
54. Mysiukiewicz O, Barczewski M, Skórczewska K, Matykiewicz D. Correlation between Processing Parameters and Degradation of Different Polylactide Grades during Twin-Screw Extrusion. Polymers 2020; 12(6): 1333.
55. Ronkay F, Molnár B, Nagy D, Szarka G, Iván B, Kristály F. Melting temperature versus crystallinity: new way for identification and analysis of multiple endotherms of poly(ethylene terephthalate). J Polym Res. 2020; 27(12): 372.
56. Batakliev T, Petrova-Doycheva I, Angelov V, Georgiev V, Ivanov E, Kotsilkova R. Effects of Graphene Nanoplatelets and Multiwall Carbon Nanotubes on the Structure and Mechanical Properties of Poly(lactic acid) Composites: A Comparative Study. Applied Sciences 2019; 9(3): 469.
57. Younus MM, Naguib HM, Fekry M, Elsawy MA. Pushing the limits of PLA by exploring the power of MWCNTs in enhancing thermal, mechanical properties, and weathering resistance. Sci Rep. 2023; 13(1): 16588.
58. Ren F, Li Z, Xu L, Sun Z, Ren P, Yan D. Large-scale preparation of segregated PLA/carbon nanotube composite with high efficient electromagnetic interference shielding and favourable mechanical properties. Composites Part B: Engineering 2018; 155: 405–413.
59. Mat Desa MSZ, Hassan A, Arsad A, Mohammad NNB. Mechanical properties of poly(lactic acid)/multiwalled carbon nanotubes nanocomposites. Materials Research Innovations 2014; 18(6): S6-14-S6-17.
60. Zou H, Yi C, Wang L, Liu H, Xu W. Thermal degradation of poly(lactic acid) measured by thermogravimetry coupled to Fourier transform infrared spectroscopy. J Therm Anal Calorim. 2009; 97(3): 929–935.